ResearchGate

See discussions, stats, and author profiles for this publication at: https://www.researchgate.net/publication/259764976

How to Determine the Size of Folding Nuclei of Protofibrils from the Concentration Dependence of the Rate and Lag-Time of Aggregation. II. Experimental Application for Insulin and...

ARTICLE *in* THE JOURNAL OF PHYSICAL CHEMISTRY B · JANUARY 2014

Impact Factor: 3.3 · DOI: 10.1021/jp4083568 · Source: PubMed

CITATIONS
4

READS
166

8 AUTHORS, INCLUDING:

Nikita V Dovidchenko
Institute of Protein Research
19 PUBLICATIONS **65** CITATIONS
SEE PROFILE

Alexey Surin
Institute of Protein Research
18 PUBLICATIONS **217** CITATIONS
SEE PROFILE

Alexei V Finkelstein
Russian Academy of Sciences
149 PUBLICATIONS **5,584** CITATIONS
SEE PROFILE

Oxana Galzitskaya
Institute of Protein Research
133 PUBLICATIONS **2,086** CITATIONS
SEE PROFILE

Available from: Alexei V Finkelstein
Retrieved on: 01 February 2016

THE JOURNAL OF PHYSICAL CHEMISTRY B

Article

pubs.acs.org/JPCB

How to Determine the Size of Folding Nuclei of Protofibrils from the Concentration Dependence of the Rate and Lag-Time of Aggregation. II. Experimental Application for Insulin and LysPro Insulin: Aggregation Morphology, Kinetics, and Sizes of Nuclei

Olga M. Selivanova,[†] Maria Yu. Suvorina,[†] Nikita V. Dovidchenko,[†] Irina A. Eliseeva,[†] Alexey K. Surin,[†,§] Alexey V. Finkelstein,[†,‡] Vadim V. Schmatchenko,[†] and Oxana V. Galzitskaya*[,†]

[†]Institute of Protein Research, Russian Academy of Sciences, 4 Institutskaya str., Pushchino, Moscow Region, 142290, Russia

[‡]Pushchino Branch of the Moscow State Lomonosov University, 4 Institutskaya str., Pushchino, Moscow Region, 142290, Russia

[§]State Research Center for Applied Microbiology & Biotechnology, Obolensk, Serpukhov District, Moscow Region, 142279, Russia

ABSTRACT: Insulin is a commonly used protein for studies of amyloidogenesis. There are a few insulin analogues with different pharmacokinetic characteristics, in particular the onset and duration of action. One of them is LysPro insulin. The behavior of LysPro insulin in the process of amyloid formation has not been studied in detail yet. To quantitatively investigate the differences between insulin and LysPro insulin in the aggregation reaction, we used thioflavin T fluorescence assay, electron microscopy, X-ray diffraction methods, and theoretical modeling. Kinetic experimental data for both insulin samples demonstrated the increase of the lag-time for LysPro insulin at low concentrations of monomers, particularly at 2 and 4 mg/mL, which corresponds to the pharmaceutical concentration. However, the morphology of insulin and LysPro insulin fibrils and their X-ray diffraction patterns is identical. Mature fibrils reach 10−12 μm in length and about 3−4 nm in diameter. The obtained analytical solution allow us to determine the sizes of the primary and secondary nuclei from the experimentally obtained concentration dependences of the time of growth and the ratio of the lag-time duration to the time of growth of amyloid protofibrils. In the case of insulin and LysPro insulin, we have exponential growth of amyloid protofibrils following the "bifurcation + lateral growth" scenario. In accord with the developed theory and the experimental data, we obtained that the size of the primary nucleus is equal to one monomer and the size of the secondary nucleus is zero in both insulin and LysPro insulin.

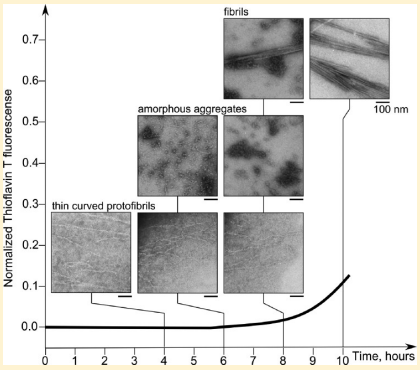

INTRODUCTION

The formation of amyloid fibrils is a case of protein misfolding, in which a protein folds into a cross-β structure instead of folding into its native structure. Experimental data demonstrate that amyloid formation depends on the amino acid sequence and is a highly specific process. A protein can become non-amyloidogenic after mutations in amyloidogenic regions, or after their complete deletion, while other mutations in these regions result in increased amyloidogenic propensity. In addition, when synthesized separately, these regions (sometimes as small as five residues long)[1] can form amyloid fibrils identical to those formed by the whole proteins.[2]

A variety of hypotheses for the mechanism of fibril formation have been proposed. There are many studies dealing with investigation of amyloid formation by various proteins under different conditions. However, no one has succeeded in designing a detailed step-by-step picture of the protein rearrangements that take place during amyloid structure formation. For some proteins, the experimental kinetic curves for processes of amyloid formation have an important feature—a lag-period, i.e., a delay before amyloid growth,[3,4] which often cannot be approximated by a quadratic function of time, as would be expected for a polymerization reaction following a simple nucleation mechanism.[5]

Here we consider human regular insulin and its analogue LysPro insulin as objects for investigation of the fibrillation process and determination of the size of the nucleus of their protofibrils. LysPro is important in the treatment of insulin-dependent diabetes because it has a more rapid onset of action. LysPro insulin has a biological effect after 42 min versus 101 min of regular insulin.[6] The duration of action of LysPro insulin is about 3 h, which is shorter than that of regular insulin (about 5 h).[7] The primary structure difference between LysPro and human insulin is the reversal of proline and lysine in the latter at positions 28 and 29 of the B chain. This reversal leads to a conformational shift in the C-end of the B chain that sterically hinders the ability of LysPro monomers to form dimers.[8] It has been proven that the C terminus of the B-chain, namely,

Received: August 21, 2013
Revised: January 14, 2014
Published: January 15, 2014

 © 2014 American Chemical Society dx.doi.org/10.1021/jp4083568 | J. Phys. Chem. B 2014, 118, 1198−1206

residues B24−B26 and B28−B29, is the crucial part of insulin for its interaction with the insulin receptor (IR) and for its self-association into dimers.[9−11] As opposed to insulin, the behavior of LysPro insulin in the process of amyloid formation has not been studied until now. Only the time of formation of amyloid fibrils under acidic conditions at 65 °C was measured, which is the same for regular human insulin and for LysPro insulin (about 5 h).[12] For insulin LysPro, it was shown by H/D exchange that the inversion of the amino acid residues in the B chain at positions B28 and B29 leads to destabilization of the C-terminus of the B chain and a more open conformation of the insulin molecule.[13]

It has been reported that insulin is secreted from the pancreas to the blood in the form of a zinc-loaded hexamer, but only the zinc-free monomer is biologically active.[14] Also, it has been shown that the fibril formation of zinc-free recombinant human insulin is faster than that of a zinc-loaded hexamer and occurs on a time scale of hours.[15,16] Besides, the human insulin fibrillation process is slower than that of the best studied bovine insulin.[17−22] Therefore, studying the fibril formation from zinc-free monomers is more advantageous than that of a zinc-loaded hexamer both for studying the lag-phase with sufficient time-resolution and the importance for insulin pharmacology.

The ability of insulin to undergo conformational changes resulting in straight fibrillar aggregates was first observed by Waugh in the 1940s.[23,24] It has been shown that insulin fibrils have common characteristics of amyloid fibrils: an elongated morphology,[25] a cross-β X-ray fibril diffraction pattern,[26−28] thioflavin T (ThT) fluorescence,[20,27] and nucleation-dependent kinetics.[22]

Despite intensive studies of fibrillogenesis of insulin, there is no generally accepted scheme for the formation of mature fibrils. The main difficulties arise in interpreting the beginning of the fibrillation process. Polymerization of insulin begins from the transition of the monomer protein from the native state to the partially unfolded conformation which can be amyloidogenic. The strong dependence of the reaction of polymerization on various external parameters leads to the formation of fibrils of insulin with different morphology, which complicates the analysis of the general scheme of fibril formation. Several models were employed to describe fibril formation by insulin, which differ by the number of monomers within the nucleus. In the first scenario, the individual insulin monomers are first denatured in solution and then directly added to the growing fibril; the size of the nucleus is not determined in these papers.[10,15,21,29] The other authors claim that a partially unfolded monomer is the nucleus for formation of a protofibril.[18,19] The second type of polymerization suggests that the precursors of protofibrils are dimers,[30−32] and three such insulin dimers form the fibrillar precursors.[30−32] In the third scenario, oligomeric structures act as nuclei for protofibril formation.[20,22,33−35] Such oligomeric structures may contain different amounts of insulin monomers (from 3 to 6) and have different morphology up to an elongated spiral that looks like a beads-on-a-string assembly of six units.[35]

The basis for the choice between different mechanisms of formation of fibrils (monomer to monomer or through the formation of various oligomers) is detection of various soluble oligomers. However, at low concentrations and at early times, reliable detection of primary aggregates is difficult. For these purposes, one uses different optical methods, such as cryo transmission electron microscopy, atomic force microscopy (AFM), and SAXS and SANS (X-ray scattering and small-angle neutron).[31,34−36] However, none of these methods is quantitative and quite reliable. Their use does not provide a complete size distribution. Results of such methods sometimes can be surprising (due to interaction of the sample with the surface and edge effects), which requires certain programs for analyzing the results and proving its statistical significance.[29] Despite the fact that all of these methods provide valuable information, none of these techniques can convincingly demonstrate how an unstable protofibrilar nucleus transforms into the stable seed for the further growth of a protofibril. Nevertheless, many experimental and theoretical models are based on the assumption that fibrils arise via nucleation (cf. ref 37).

Therefore, the question about the size of nuclei of protofibrils formed by insulin is still open despite the large number of papers dealing with this question. The analytical solution of the suggested kinetic model of the process of formation of amyloid protofibrils is considered in our first paper of the series[38] which allows us to calculate the size of the primary nucleus of protofibrils from the experimentally obtained concentration dependences of the ratio of the lag-time to the time of growth of amyloid fibrils and the size of the secondary nucleus from the experimentally obtained concentration dependences of the time of growth of amyloid fibrils. In the case of insulin and LysPro insulin, we observed exponential growth of amyloid fibrils following the "bifurcation + lateral growth" scenario. In accord with the developed theory[38] and the experimental data, we obtained that the size of the primary nucleus is equal to one monomer and the size of the secondary nucleus is zero in both insulin and LysPro insulin.

EXPERIMENTAL METHODS

Sample Preparation. Zinc-free recombinant human insulin and insulin analogue LysPro were obtained from "Gerofarm-Bio" (Obolensk, Russia) and were checked by the tandem mass spectrometry technique (LCQ Deca XP, Thermo Finnigan, USA). The solutions of human insulin and analogue LysPro, 2−15 mg/mL, were prepared fresh before use in 20% acetic acid (pH 2.0) with 140 mM sodium chloride and centrifuged (5 min, 12000 rpm); no agitation was used in all of our experiments. The concentrations of insulin and its analogue were determined by absorbance at 276 nm, using the extinction coefficient of 1.0 for 1 mg/mL.[22]

Thioflavin T Fluorescence Assay. Free ThT has excitation and emission maxima at ∼350 and ∼450 nm, respectively (upon binding to fibrils, the excitation and emission λ_{max} change to ∼450 and ∼485 nm, respectively). A stock solution of ThT was prepared at a concentration of 20 or 50 mM in 20% acetic acid (pH 2.0) and 140 mM NaCl and stored at 4 °C protected from light. For ThT fluorescence measurements, ThT was added to the protein sample up to the molar ratio 3.5/1.[39] ThT is present in the sample during the whole fibril formation reaction. ThT fluorescence measurements were carried out on a Cary Eclipse fluorescence spectrophotometer (Varian, Australia) at 37 °C.

Electron Microscopy. Solutions of monomeric human insulin and LysPro insulin, 2 mg/mL, were freshly prepared in 20% acetic acid (pH 2.0) containing sodium chloride (140 mM) and heated at 37 °C for 3 days. Sample aliquots were collected at different times (every hour for 11 h, after 24 h, and after 3 days). The samples were dissolved in the same solution to 0.2 mg/mL before studying with electron microscopy. A Formvar-coated copper grid (400 mesh) was placed on a 10 μL

dx.doi.org/10.1021/jp4083568 | J. Phys. Chem. B 2014, 118, 1198−1206

sample. After 5 min, the grid was negatively stained with 1% (w/v) aqueous uranyl acetate for 1−1.5 min and then examined under transmission electron microscopy (JEM-100C) at an accelerating voltage of 80 kV.

X-ray Diffraction. After 3 days of incubation at 37 °C, insulin fibrils (in 100 μL of 20% acetic acid (pH 2.0), 140 mM NaCl, 2 mg/mL) were centrifuged at 12000 × g for 5 min. Two methods were used for sample preparation. In the first case, fibrils were suspended in 5 μL of the same solution. A drop of the fibril solution was placed between the wax-sealed ends of two glass tubes (a 1 mm diameter) separated by 2 mm and allowed to dry. In the second case, to remove the salts, the fibrils were washed by 100 μL of water (Milli-Q) and centrifuged at 12000 × g for 5 min; after that, 5 μL of the washed fibril solution was placed between two glass tubes and allowed to dry.[40] After drying for 30−40 min, rod specimens 1.5 mm long and about 0.1 mm in diameter were obtained. The fiber diffraction images were collected on a Microstar X-ray generator with HELIOX optics equipped by a Platinun135 CCD detector (X8 Proteum system, Bruker AXS) at the Institute of Protein Research, RAS, Pushchino. Cu Kα radiation (λ = 1.54 Å) was used. The samples were oriented perpendicular to the X-ray beam using a 4-axis kappa goniometer.

Fluorescence Microscopy. For analysis of the samples (with 4−8 mg/mL of insulin) with FM, thioflavin T was added until a final concentration of 25−75 μM. A drop of insulin solution was placed between a slide glass and a cover glass, which were then glued together to minimize evaporation. The thioflavin T was excited using the 405 nm laser. The emission was measured at 450−550 nm. The images and sections of the fibrils were obtained using a confocal microscope TCS SPE DM2500 and the LAS AF Version 2.1.0 built-in 4316 software (Leica Microsystems GmbH, Germany).

RESULTS

The aim of this paper is to determine the size of folding nuclei of protofibrils for insulin and LysPro insulin and to find the difference in behavior of both molecules in the fibrillation process. To estimate the size of folding nuclei of protofibrils by using the theory suggested in the first paper of this series,[38] we should obtain concentration dependences of the time of growth and the ratio of the lag-time to the time of growth of amyloid fibrils by considering kinetic curves of ThT fluorescence, and to determine the mechanism of the exponentional[4] fibril formation (that, in principle,[38] can be a "growth from the surface", "fragmentation", or "bifurcation") by direct visualization of the amyloid fibril formation using electron microscopy and X-ray diffraction.

Insulin and LysPro Insulin Polymerization by Electron Microscopy and Fluorescence Microscopy Analysis. For electron microscopy (EM) investigations, both types of insulin were used at a concentration of 0.2 mg/mL. Sample aliquots were collected at desired intervals of time (every hour during the first 11 h, at 24 h, and after 3 days). According to the EM data, polymerization of human insulin is not observed up to the first 3 h of incubation. After 3−5 h, curved elongated particles (up to 400 nm long and less than 3 nm in width) appeared (see Figure 1). We consider these extended formations as protofibrils.[41] The quantity of protofibrils increased up to 6 h of incubation. At the same time, amorphous aggregates of different sizes occurred. Therefore, there are two kinds of aggregates (thin curved protofibrils and amorphous aggregates)

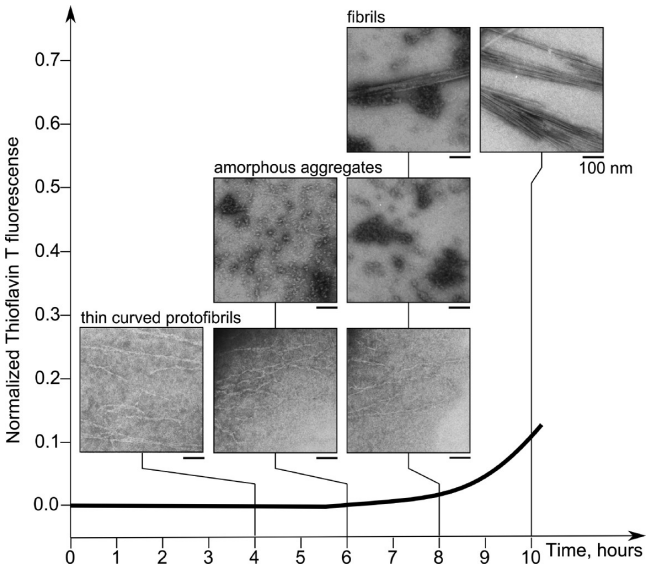

Figure 1. Overlapping of electron microscopy images and normalized ThT fluorescence data for lag-time of the initial stage of insulin polymerization up to 10 h at a concentration of 2 mg/mL. The scale bar is 100 nm.

before the formation of mature fibrils. After 6−8 h of incubation, the first thick insulin fibrils appeared. After 6−8 h of incubation, protofibrils, amorphous aggregates, and insulin fibrils can be observed simultaneously in the insulin samples (Figure 1). Thus, the mature protein fibrils appeared only after 8 h of insulin incubation, while the amount of intermediate protofibrils decreased, and amorphous aggregates almost disappeared. Active polymerization of insulin occurs up to 10−11 h of incubation. This is accompanied by elongation of the fibrils for both samples up to 10−12 μm. The fibrils interact laterally with each other, resulting in the formation of big clusters composed from ribbons, bundles, and twisting bundles (Figure 2). Protein aggregation is the result of increasing the incubation time up to 24 h. According to the EM data, the number of large fibril clusters increases in the samples after 24 h and 3 days of incubation, but the length of the fibrils does not change (remains about 10−12 μm). The samples of the mature fibrils after 3 days of incubation were kept at room temperature.

The kinetics of growth of fibrils was observed also with a fluorescent microscope (FM). This method allows, in contrast to the EM analysis, one to measure more accurately the length of the mature fibrils. Insulin fibrils were prepared at a concentration of 4 mg/mL for boosting the kinetics (Figure 3). Figure 3 shows a comparison of the two methods of observation. FM allows one to see the process in general and EM to analyze the processes occurring in the solution during insulin fibrillation with more details and to see the morphology of aggregates and of insulin fibrils.

It should be noted that the morphologies of insulin and LysPro insulin fibrils are identical. However, the lag-time of fibril formation (at 2 and 4 mg/mL) for LysPro insulin is 5 h more than that for insulin. One can see the fibrils with a diameter of 3−4 nm at the end of the lag-period, which is in good agreement with the data reported in the previous studies.[22,26,41−43] These fibrils are associated with each other laterally (superfibrillar aggregation of fibrils), and fibrils in bundles with smooth edges are often observed (they are clearly visible on short fibrils, Figure 3c). In these bundles, the

dx.doi.org/10.1021/jp4083568 | J. Phys. Chem. B 2014, 118, 1198−1206

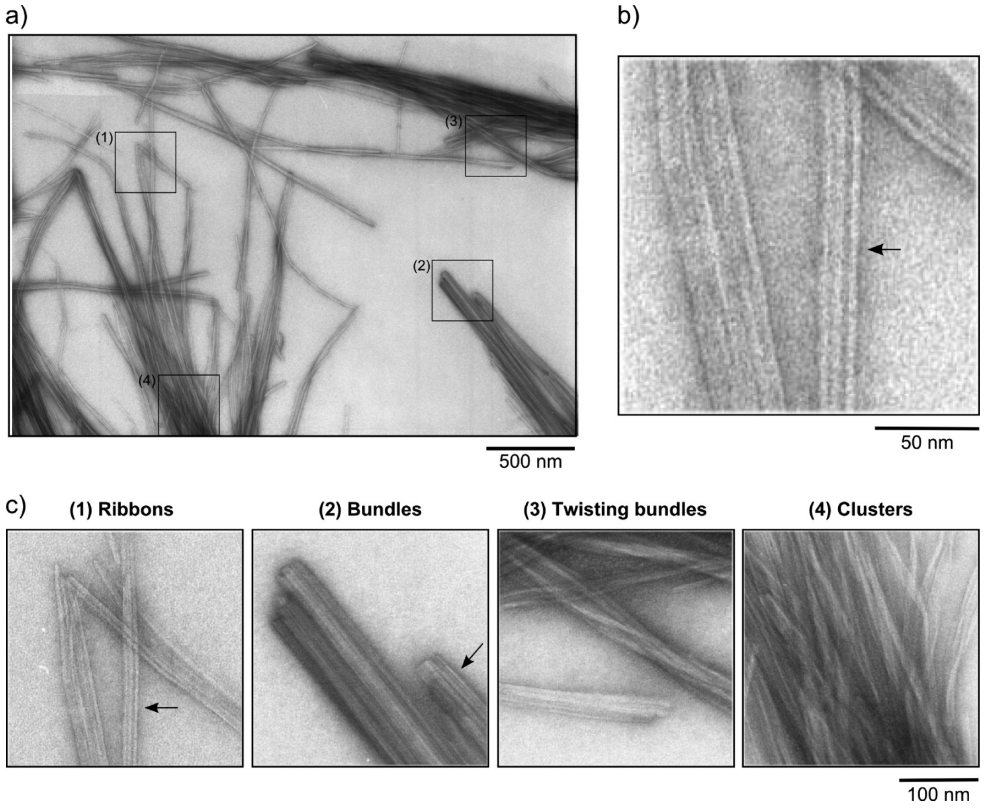

Figure 2. Electron microscopy images of human insulin at a concentration of 2 mg/mL: (a) general view (field) of human insulin after 24 h of incubation; (b) image of a ribbon-like type of lateral interactions of insulin fibrils at higher magnification. (c) Gallery of types of lateral interactions of insulin fibrils. Arrows indicate fibrils with a diameter of ~3−4 nm.

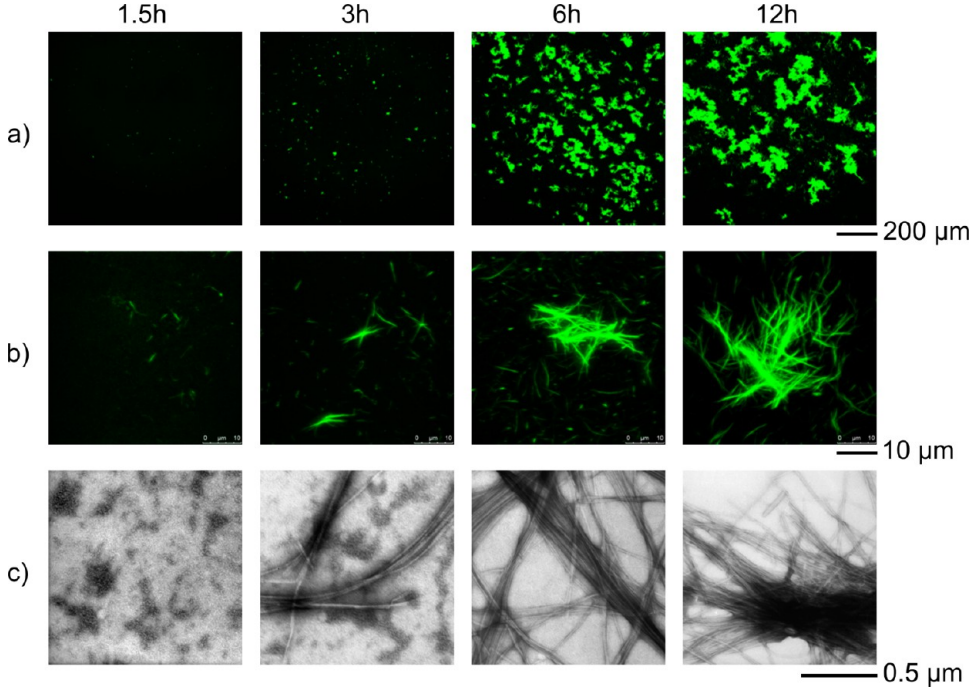

Figure 3. Observation of the kinetics of growth of insulin fibrils by electron microscopy (EM) and fluorescent microscopy (FM): (a and b) FM at different magnification; (c) EM. Experiments are carried out for 12 h at an insulin concentration of 6 mg/mL.

individual fibrils are evenly distributed and have the same length. This may indicate that a single fibril forms a surface that provokes almost immediate formation of consequent protofibrils onto it. Our conclusion is consistent with the data of Jansen et al.,[18] that individual protofibrils/fibrils may play the role of a matrix or platform onto which small insulin particles (monomers or oligomers) are associated. After EM studies, we can conclude that insulin and LysPro insulin fibril formation

dx.doi.org/10.1021/jp4083568 | J. Phys. Chem. B 2014, 118, 1198−1206

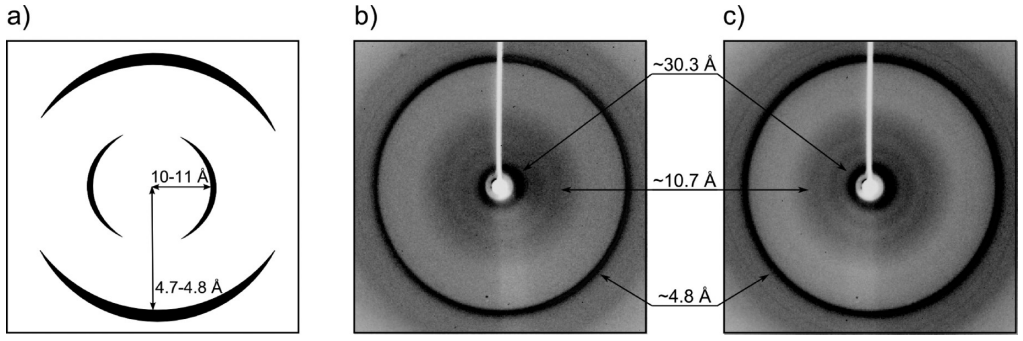

Figure 4. X-ray diffraction patterns of insulin fibrils. The samples were prepared in 20% acetic acid (pH 2.0) containing 140 mM NaCl and before X-ray diffraction investigations were washed with water (see the Experimental Methods). (a) Schematic image of a typical diffraction picture of amyloid fibrils; (b) insulin; (c) LysPro insulin.

occurs by the lateral growth, or rather "bifurcation + lateral growth" scenario. Mathematical description of such a scenario is identical to the description of the mechanism of "bifurcation" (see paper I, DOI 10.1021/jp4083294).

X-ray Diffraction. An important feature of fibril structures is the presence of a specific X-ray diffraction pattern where the 4.8 and 11 Å reflections correspond to the cross-β structure (Figure 4a).[28] According to our X-ray diffraction data, insulin and LysPro insulin give identical diffraction patterns. Three reflections can be observed in Figure 4: sharp and intensive reflection at 4.8 Å and two weaker and more diffuse reflections at ~11 and ~30 Å, respectively. The reflections at 4.8, 11, and 30 Å for insulin are in good agreement with the data reported previously.[26,30,44,45] The data for LysPro insulin were obtained by us for the first time. The meridian reflection at 4.8 Å corresponds to the distance between strands in the β-sheet, and the β-strands are oriented perpendicularly to the fibril axis. The 10−11 Å equator reflection arises from the spacing between β-sheets oriented parallel to the fibril axis. The 30 Å equator reflection may correspond to the distance between laterally spaced fibrils with a diameter of 3 nm. A similar assumption was made previously.[26,44] It is noteworthy that insulin and LysPro insulin have their individual specific fingerprints with an additional X-ray diffraction reflection corresponding to 30 Å (3 nm), which reflects the structural features of their fibrils (see Figure 4b,c), which are not similar to those of the other amyloid protein fibrils whose average diameter is about 10 nm (see Figure 4a).[46]

Kinetic Curves of ThT Fluorescence. The ThT fluorescence as a function of incubation time is presented in Figure 5 for samples of insulin (a) and LysPro insulin (b) at concentrations of 2, 4, 6, 8, 10, and 15 mg/mL at 37 °C in 20% acetic acid (pH 2.0) containing 140 mM NaCl (i.e., conditions where insulin is known to be monomeric).[20] The figure indicates that the increase in ThT fluorescence intensity, in a wide range of protein concentration (2−15 mg/mL), follows the typical sigmoid pattern at all concentrations and has common features (look like a classical three-step curve—showing the nucleation (with lag-time), elongation, and maturation phases of fibril formation). However, the lag-time values decrease with increasing insulin concentration and almost do not change at insulin concentrations of 10−15 mg/mL, which agrees with the data of Fodera et al.[47] It should be noted that one can see changes in the kinetic profiles between insulin and LysPro insulin at relatively low insulin concentrations, particularly at 2 and 4 mg/mL. At 2 mg/mL, the lag-phase of insulin and LysPro insulin varies from 7 to 12 h, and at

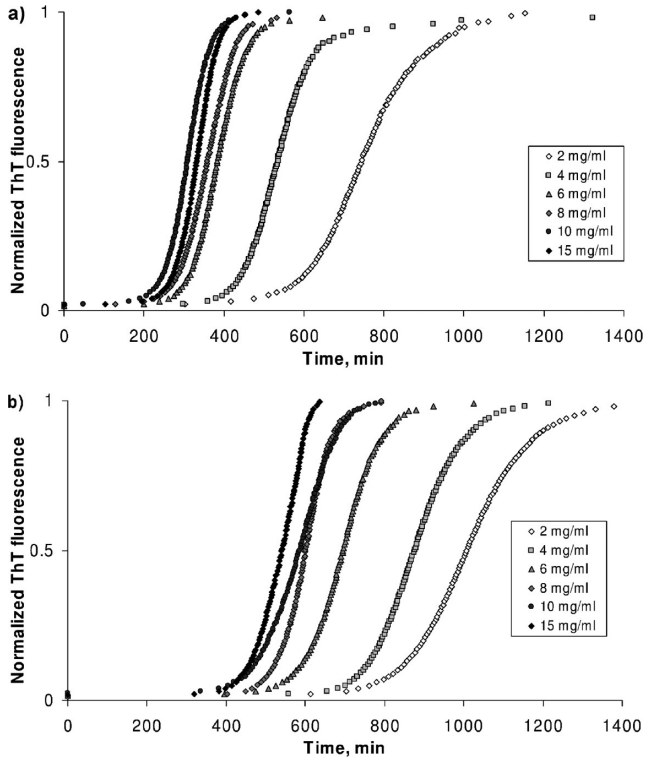

Figure 5. ThT fluorescence data for insulin (a) and LysPro insulin (b) presented as a function of incubation time at different insulin concentrations. For each concentration, 4−5 experiments have been done (each normalized to the time of reaching 50% of the maximal ThT fluorescence).

4 mg/mL, from 5 to 10 h, correspondingly. According to the earlier investigations[13] using the H/D exchange, LysPro insulin has a more open conformation in solution than regular human insulin.

According to our theory,[38] one can distinguish some mechanism of growth on the basis of kinetic data. Thus, the small (<0.2) value of L_{rel} (the lag-time to the growth time ratio) together with independence of L_{rel} on the total concentration $[M_\Sigma]$ of protein in solution determines applicability of the linear regime of growth, and in the case of inapplicability of the latter consideration of the exponential mechanism of growth is required. As it can be clearly seen from Figures 5 and 6, we have $L_{rel} \approx 2-3$, which means that it is definitely an exponential growth scenario for both insulins. One can roughly define three types of possible mechanisms of exponential growth: growth

dx.doi.org/10.1021/jp4083568 | J. Phys. Chem. B 2014, 118, 1198−1206

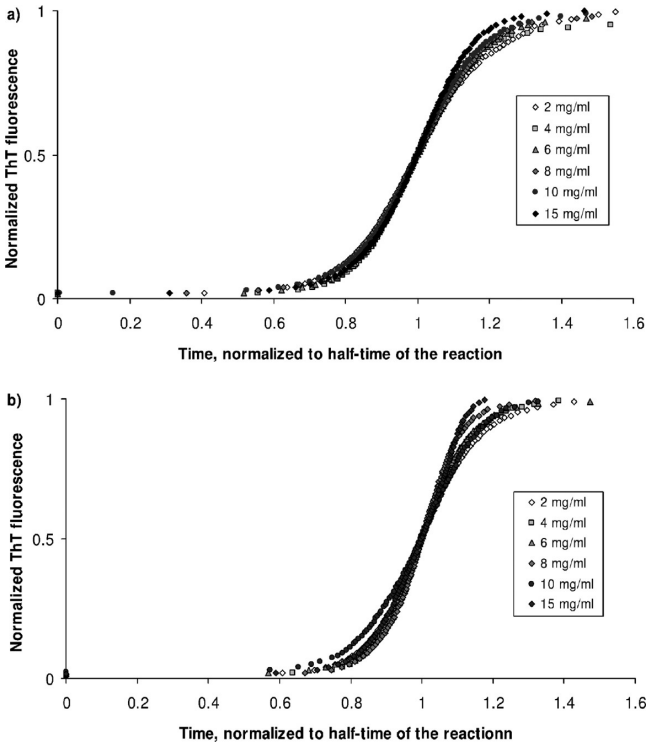

Figure 6. ThT fluorescence of insulin (a) and LysPro insulin (b) represented from Figure 5 as a function of incubation time normalized to the time of reaching 50% of the maximal ThT fluorescence.

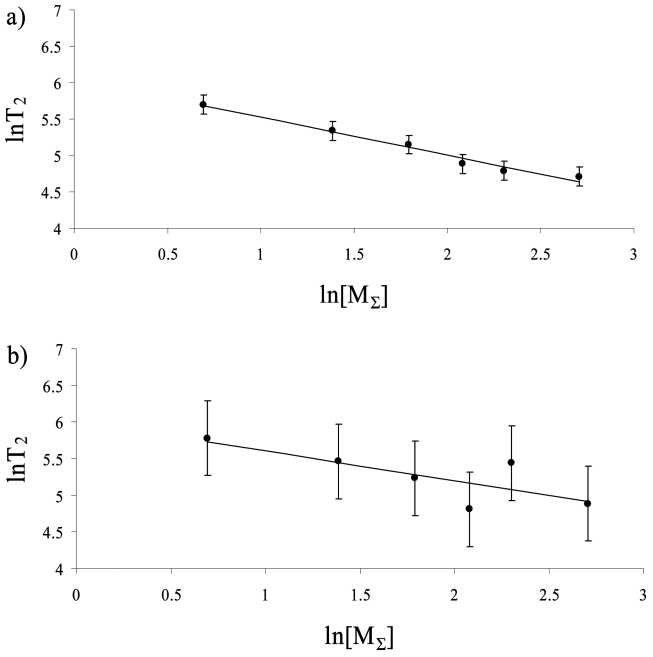

Figure 7. The approximation line calculated by the least-squares method plotted in coordinates ($\ln T_2$, $\ln[M_\Sigma]$) for (a) insulin and (b) LysPro insulin. The tangent coefficient $d(\ln T_2)/d(\ln[M_\Sigma])$ of the approximation line is -0.52 ± 0.13 in the case of insulin and -0.40 ± 0.51 in the case of LysPro insulin (see explanation in the text; the errors are computed using the Student's coefficient corresponding to 0.95 confidence level). This means that the obtained $d(\ln T_2)/d(\ln[M_\Sigma])$ value is significantly closer to 0.5 than to 0 or 1 in both cases. This value ($\approx$0.5) is inconsistent with the "growth from the surface" but consistent with the "linear growth" (which, though, should have $L_{rel} < 0.2$, inconsistent with Figure 8), "fragmentation" (which, though, is inconsistent with Figures 1 and 2), and bifurcation, with the secondary nucleus size $n_2 = 0$, or, in any case, with n_2 which is significantly closer to 0 than to +1 or −1 (see Table 1 in ref 38).

from the surface, bifurcation, and fragmentation. Despite the difference of the processes, in kinetic experiments, fragmentation and bifurcation show a very similar behavior if the size of the secondary nucleus is equal to zero. According to our theory, there is no chance to distinguish between these two scenarios of exponential growth without direct experiments demonstrating what exact scenario takes place in the given case. However, the behavior of kinetic dependencies in the case of growth from the surface scenario differs from that in the fragmentation/bifurcation scenario.[38]

One of the conclusions that can be made from our theory is that the dependence of $\ln T_2$ (T_2 being the transition time, see Figure 1 in ref 38) on $\ln[M_\Sigma]$ in the case of exponential growth must be linear, and moreover, in the case of growth from the surface, its tangent coefficient $k = d(\ln T_2)/d(\ln[M_\Sigma])$ must be -1, while in the case of the bifurcation scenario (in our case, the branching process was determined to be the primary one; see the discussion of the results on EM data) it must be $-(n_2 + 1)/2$, where n_2 is the size of the secondary nucleus (see Table 1 of ref 38).

As can be seen from Figure 7, the experiments support our theory, resulting in linear dependence of $\ln T_2$ on $\ln[M_\Sigma]$. Calculations of the tangent coefficient give -0.52 ± 0.13 for insulin and -0.40 ± 0.51 for LysPro insulin, which means that, according to our theory, $n_2 = -1 - 2[d(\ln T_2)/d(\ln[M_\Sigma])]$ is very close to zero for the "bifurcation" scenario.

Modeling of Insulin Amyloid Formation. In our first paper from this series,[38] we demonstrated that the linear growth model can be applied only when $L_{rel} < 0.2$, where L_{rel} is the ratio of the lag-period time to the characteristic time of transition of protein molecules into amyloid aggregates. Figures 5, 6, and 8 show that the kinetics of formation of insulin and LysPro insulin amyloids is exponential because L_{rel} is about 2 and 3, correspondingly. It should be noted that the first who noticed such behavior of kinetics of amyloidogenesis for insulin was Fodera et al.[47] We found $\langle L_{rel} \rangle$ for the kinetic data from that work to be ~5, which is not equal to L_{rel} that we get in our experiments, but it could be addressed to different experiment conditions. We analyzed data from Fodera's work in paper I (DOI 10.1021/jp4083294) and obtained $n_2 = -0.48 \pm 0.16$ (i.e., the size of the secondary nucleus is close to zero) and $n^* = 1.13 \pm 0.19$ (i.e., the size of the primary nucleus close to 1). From EM data (Figure 1), we can see that the insulin protofibrils have the points of growth situated along the length of the growing fibril, which lead to the formation of a fibrillar amyloid layer. This scenario is a form of the bifurcation scenario of amyloid aggregate growth which was reported recently for glucagon and Aβ42 peptide.[48−50] From the dependence of $\ln T_2$ on $\ln[M_\Sigma]$, we obtained that the size of the secondary nucleus is zero, which means that the initiation energy is connected with deformation of the protofibril rather than with the deformation of the adhering monomer. Moreover, a comparison of L_{rel} obtained in the experiments with different protein concentrations showed that L_{rel} is virtually independent of the concentration of insulin and LysPro monomers (Figures 6 and 8). According to our theory, for the bifurcation scenario (see Table 1 in ref 38), $L_{rel} = \text{const}' - (n^* - n_2 - 1) \ln[M_\Sigma]$ for bifurcation, where $[M_\Sigma]$ is the initial concentration of monomers, n_2 is the size of the

dx.doi.org/10.1021/jp4083568 | J. Phys. Chem. B 2014, 118, 1198−1206

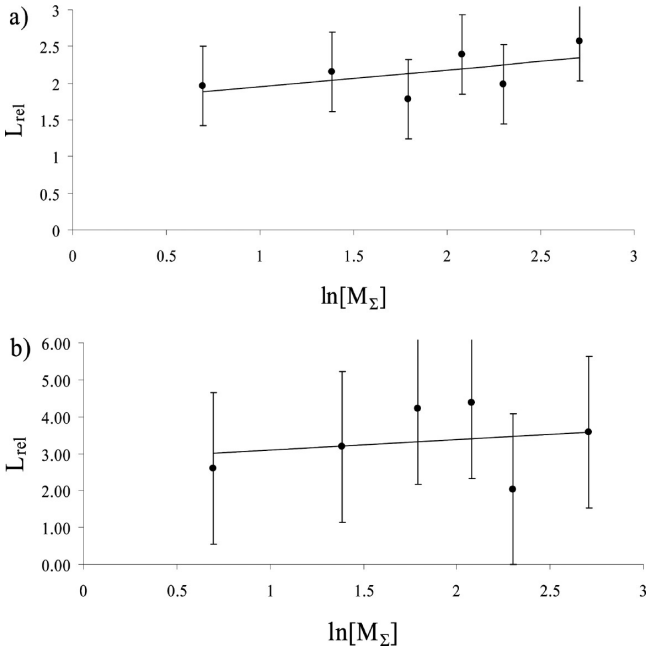

Figure 8. The approximation line calculated by the least-squares method plotted in coordinates (L_{rel}, $\ln[M_\Sigma]$) for (a) insulin and (b) LysPro insulin. The tangent coefficient of the approximation line, $d(L_{rel})/d(\ln[M_\Sigma])$, is 0.23 ± 0.52 in the case of insulin and 0.29 ± 1.98 in the case of LysPro insulin (see explanation in the text; the errors are computed using the Student's coefficient corresponding to 0.95 confidence level).

secondary nucleus, and n^* is the size of the primary nucleus (i.e., the number of monomers in the most unstable intermediate of the growing protofibril).

Thus, the virtual independence of L_{rel} on $[M_\Sigma]$, as in the case of insulin or LysPro insulin, is possible only if the size of the primary nucleus n^* is close to 1. This result can be verified by a direct calculation of n^* from the experimental data by plotting the experimental points in the coordinates (L_{rel}, $\ln[M_\Sigma]$) (see Figure 8). Given $n^* = 1 + n_2 - d(L_{rel})/d(\ln[M_\Sigma])$, one easily obtains (with n_2 taken from the legend to Figure 7) that $n^* = 0.81 \pm 0.54$ for insulin and $n^* = 0.51 \pm 2.05$ for LysPro insulin.

DISCUSSION

The kinetics of insulin fibril formation (and that of other amyloidogenic proteins) is influenced by many environmental factors. These include protein concentration, pH, ionic strength, the presence and relative concentrations of various anions and cations, the presence of denaturing agents (urea, guanidine chloride) or stabilizers (sucrose), temperature, and agitation.[22,24,26]

Depending on the conditions, insulin may be present in solution as monomers, dimers, and hexamers. The protein is predominantly monomeric in 20% acetic acid (pH 2.0), dimeric in 20 mM HCl, and hexameric at pH 7.5 in the presence of zinc.[22,24,26,34,51,52] The morphology of insulin fibrils depends on the conditions of their formation. According to EM and atomic force microscopy (AFM), the diameter of fibrils varies from 3 to 15 nm and the fibril lengths are several micrometers.[10,21,25,26,41,43,44,53,54]

According to the published data,[20,22,33,34] insulin fibril formation occurs by a simplified scheme: hexamer − monomer − fibril (which perfectly fits to results of our study). The study of insulin fibrillation in 20% acetic acid shows that the formation of fibrils requires significant structural changes in the native molecule,[34] leading to an amyloidogenic protein conformation.[55]

According to our EM data, under the chosen conditions, straight, laterally arranged fibrils of insulin with a diameter of about 3−4 nm almost always appear. According to the data obtained by ES-DMA, the minimum component size of insulin fibrils is 2.8 ± 0.3 nm, which corresponds to that of the monomer protein.[29] In addition, earlier Nielsen et al.,[20] using AFM, showed that the diameter of individual fibrils/protofibrils is about 2.1 nm. Using the same method, Khurana et al.[41] presented a model of insulin fibril assembly, where the diameter of protofibrils is 1.9 ± 0.3 nm and the diameter of fibrils is 3 ± 0.4 nm. The earliest reported measured distance between laterally spaced insulin fibrils was 4 nm, as reported in ref 26. The diameter of about 3−4 nm obtained from our experimental data for separate fibrils allows suggesting that a single fibril consists of two or one protofibrils, which may be formed from monomers of insulin. This conclusion is consistent with the above-mentioned data.[20,26,29,41,43] The diameter of about 3−4 nm does not match the rounded shape oligomers consisting of 5−6 particles of protein: such oligomers typically have a diameter of 10 nm or more and are often observed during the lag-phase for many amyloidogenic proteins.[46] Nevertheless, other polymerization conditions (as compared to our experimental conditions) for insulin result in the formation of wider, twisted fibrils with diameters ranging from 5 to 20 nm.[10,21,25,26,41,43,44,53,54] Since LysPro does not form dimers[56] and the width of LysPro insulin fibrils corresponds to the size of the insulin molecule,[10] it is highly probable that the formation of insulin and LysPro insulin fibrils goes through attachment of monomers.

Among possible scenarios suggested in the literature (see the Introduction section), we have determined that insulin and LysPro insulin fibril formation occurs according to the "bifurcation + lateral growth along the surface of fibrils" scenario, the mathematical description of which is identical to the description of the mechanism of "bifurcation" (see paper I, DOI 10.1021/jp4083294). According to this scenario, individual insulin monomers are first denatured in solution and then directly added to the growing protofibril. The size of the primary nucleus is one monomer, and the size of the secondary nucleus is zero. It should be noted that the nucleus is the most unstable intermediate of the growing protofibril and could not be seen directly by any experimental method. Probably the authors of ref 35 observed a seed (a beads-on-a-string assembly of six units), which is the smallest stable protofibril of any kind. It should be stressed that the true pathway of the amyloid formation can be different from that traced by the appearance of different observable intermediate structures, because the observable structures are only stable structures and can be out-of-pathway dead-ends, while the on-pathway structures can be unstable and not observable directly (like the nucleus, i.e., the most unstable but unavoidable folding intermediate). If the number of monomers involved in the early aggregates is negligible as compared to that in solution (which is suggested by our experiments, see Figure 3), it will not affect significantly the behavior of kinetic curves.

CONCLUSIONS

In order to obtain a deeper understanding of the insulin fibrillation process, experimental and theoretical approaches have been combined in this study. In addition to the amyloid

dx.doi.org/10.1021/jp4083568 | J. Phys. Chem. B 2014, 118, 1198−1206

fibrillogenesis of zinc-free recombinant human insulin, the amyloid fibrillogenesis of the LysPro human analogue insulin (LysPro insulin) has been investigated for the first time by ThT fluorescence, electron microscopy, X-ray diffraction, and theoretical modeling. According to ThT fluorescence and EM data, human regular insulin and LysPro insulin have different lag-times of fibril formation (especially at 2−4 mg/mL). The morphology of both regular and LysPro human insulin fibrils is identical. In the case of insulin and LysPro insulin, we observed exponential growth of amyloid fibrils following the "bifurcation + lateral growth" scenario. In accord with the developed theory[38] and the experimental data, we obtained that the size of the primary nucleus is equal to one monomer and the size of the secondary nucleus is zero in both insulin and LysPro insulin. The knowledge of the lag-phase period can help to guide an important medical task of developing insulin analogues with pharmacokinetic characteristics different from those of regular insulin, and in particular analogues with a longer lag-phase of amyloid formation.

AUTHOR INFORMATION

Corresponding Author

*E-mail: ogalzit@vega.protres.ru. Phone/fax: +74967-318275/ +74967-318435.

Notes

The authors declare no competing financial interest.

ACKNOWLEDGMENTS

We are grateful to A. D. Nikulin and M. A. Stoylov for assistance in some experiments and T. B. Kuvshinkina and D. Reifsnyder for assistance in preparation of the paper. This study was supported in part by the Russian Foundation for Basic Research (Grant No. 13-04-00253a), Russian Academy of Sciences (programs "Molecular and Cell Biology" (Grant Nos. 01201353567 and 01201358029) and "Fundamental Sciences to Medicine").

REFERENCES

(1) Lopez de la Paz, M.; Serrano, L. Sequence Determinants of Amyloid Fibril Formation. *Proc. Natl. Acad. Sci. U.S.A.* **2004**, *101*, 87−92.

(2) Thompson, A.; White, A. R.; McLean, C.; Masters, C. L.; Cappai, R.; Barrow, C. J. Amyloidogenicity and Neurotoxicity of Peptides Corresponding to the Helical Regions of Prp(C). *J. Neurosci. Res.* **2000**, *62*, 293−301.

(3) Knowles, T. P.; Waudby, C. A.; Devlin, G. L.; Cohen, S. I.; Aguzzi, A.; Vendruscolo, M.; Terentjev, E. M.; Welland, M. E.; Dobson, C. M. An Analytical Solution to the Kinetics of Breakable Filament Assembly. *Science* **2009**, *326*, 1533−1537.

(4) Xue, W. F.; Homans, S. W.; Radford, S. E. Systematic Analysis of Nucleation-Dependent Polymerization Reveals New Insights into the Mechanism of Amyloid Self-Assembly. *Proc. Natl. Acad. Sci. U.S.A.* **2008**, *105*, 8926−8931.

(5) Oosawa, F.; Asakura, S.; Hotta, K.; Imai, N.; Ooi, T. G-F Transformation of Actin as a Fibrous Condensation. *J. Polym. Sci.* **1959**, *37*, 323−336.

(6) Howey, D. C.; Bowsher, R. R.; Brunelle, R. L.; Woodworth, J. R. [Lys(B28), Pro(B29)]-Human Insulin. A Rapidly Absorbed Analogue of Human Insulin. *Diabetes* **1994**, *43*, 396−402.

(7) Holleman, F.; van den Brand, J. J.; Hoven, R. A.; van der Linden, J. M.; van der Tweel, I.; Hoekstra, J. B.; Erkelens, D. W. Comparison of Lysb28, Prob29-Human Insulin Analog and Regular Human Insulin in the Correction of Incidental Hyperglycemia. *Diabetes Care* **1996**, *19*, 1426−1429.

(8) Holleman, F.; Hoekstra, J. B. Insulin Lispro. *N. Engl. J. Med.* **1997**, *337*, 176−183.

(9) Antolikova, E.; Zakova, L.; Turkenburg, J. P.; Watson, C. J.; Hanclova, I.; Sanda, M.; Cooper, A.; Kraus, T.; Brzozowski, A. M.; Jiracek, J. Non-Equivalent Role of Inter- and Intramolecular Hydrogen Bonds in the Insulin Dimer Interface. *J. Biol. Chem.* **2011**, *286*, 36968−36977.

(10) Brange, J.; Dodson, G. G.; Edwards, D. J.; Holden, P. H.; Whittingham, J. L. A Model of Insulin Fibrils Derived from the X-Ray Crystal Structure of a Monomeric Insulin (Despentapeptide Insulin). *Proteins* **1997**, *27*, 507−516.

(11) Brange, J.; Ribel, U.; Hansen, J. F.; Dodson, G.; Hansen, M. T.; Havelund, S.; Melberg, S. G.; Norris, F.; Norris, K.; Snel, L.; et al. Monomeric Insulins Obtained by Protein Engineering and Their Medical Implications. *Nature* **1988**, *333*, 679−682.

(12) Huang, K.; Dong, J.; Phillips, N. B.; Carey, P. R.; Weiss, M. A. Proinsulin Is Refractory to Protein Fibrillation: Topological Protection of a Precursor Protein from Cross-Beta Assembly. *J. Biol. Chem.* **2005**, *280*, 42345−42355.

(13) Ramanathan, R.; Gross, M. L.; Zielinski, W. L.; Layloff, T. P. Monitoring Recombinant Protein Drugs: A Study of Insulin by H/D Exchange and Electrospray Ionization Mass Spectrometry. *Anal. Chem.* **1997**, *69*, 5142−5145.

(14) Cahill, G. F., Jr. The Banting Memorial Lecture 1971. Physiology of Insulin in Man. *Diabetes* **1971**, *20*, 785−799.

(15) Brange, J.; Andersen, L.; Laursen, E. D.; Meyn, G.; Rasmussen, E. Toward Understanding Insulin Fibrillation. *J. Pharm. Sci.* **1997**, *86*, 517−525.

(16) Hua, Q. X.; Weiss, M. A. Mechanism of Insulin Fibrillation: The Structure of Insulin under Amyloidogenic Conditions Resembles a Protein-Folding Intermediate. *J. Biol. Chem.* **2004**, *279*, 21449−21460.

(17) Dzwolak, W.; Ravindra, R.; Lendermann, J.; Winter, R. Aggregation of Bovine Insulin Probed by Dsc/Ppc Calorimetry and Ftir Spectroscopy. *Biochemistry* **2003**, *42*, 11347−11355.

(18) Jansen, R.; Dzwolak, W.; Winter, R. Amyloidogenic Self-Assembly of Insulin Aggregates Probed by High Resolution Atomic Force Microscopy. *Biophys. J.* **2005**, *88*, 1344−1353.

(19) Loksztejn, A.; Dzwolak, W. Vortex-Induced Formation of Insulin Amyloid Superstructures Probed by Time-Lapse Atomic Force Microscopy and Circular Dichroism Spectroscopy. *J. Mol. Biol.* **2010**, *395*, 643−655.

(20) Nielsen, L.; Frokjaer, S.; Brange, J.; Uversky, V. N.; Fink, A. L. Probing the Mechanism of Insulin Fibril Formation with Insulin Mutants. *Biochemistry* **2001**, *40*, 8397−8409.

(21) Nielsen, L.; Frokjaer, S.; Carpenter, J. F.; Brange, J. Studies of the Structure of Insulin Fibrils by Fourier Transform Infrared (Ftir) Spectroscopy and Electron Microscopy. *J. Pharm. Sci.* **2001**, *90*, 29−37.

(22) Nielsen, L.; Khurana, R.; Coats, A.; Frokjaer, S.; Brange, J.; Vyas, S.; Uversky, V. N.; Fink, A. L. Effect of Environmental Factors on the Kinetics of Insulin Fibril Formation: Elucidation of the Molecular Mechanism. *Biochemistry* **2001**, *40*, 6036−6046.

(23) Waugh, D. F. The Linkage of Corpuscular Protein Molecules. I. A Fibrous Modification of Insulin. *J. Am. Chem. Soc.* **1944**, *66*, 663−663.

(24) Waugh, D. F. A Fibrous Modification of Insulin. I. The Heat Precipitate of Insulin. *J. Am. Chem. Soc.* **1946**, *68*, 247−250.

(25) Jimenez, J. L.; Nettleton, E. J.; Bouchard, M.; Robinson, C. V.; Dobson, C. M.; Saibil, H. R. The Protofilament Structure of Insulin Amyloid Fibrils. *Proc. Natl. Acad. Sci. U.S.A.* **2002**, *99*, 9196−9201.

(26) Burke, M. J.; Rougvie, M. A. Cross- Protein Structures. I. Insulin Fibrils. *Biochemistry* **1972**, *11*, 2435−2439.

(27) Groenning, M.; Norrman, M.; Flink, J. M.; van de Weert, M.; Bukrinsky, J. T.; Schluckebier, G.; Frokjaer, S. Binding Mode of Thioflavin T in Insulin Amyloid Fibrils. *J. Struct. Biol.* **2007**, *159*, 483−497.

(28) Sunde, M.; Blake, C. The Structure of Amyloid Fibrils by Electron Microscopy and X-Ray Diffraction. *Adv. Protein Chem.* **1997**, *50*, 123−159.

(29) Pease, L. F., 3rd; Sorci, M.; Guha, S.; Tsai, D. H.; Zachariah, M. R.; Tarlov, M. J.; Belfort, G. Probing the Nucleus Model for Oligomer Formation During Insulin Amyloid Fibrillogenesis. *Biophys. J.* **2010**, *99*, 3979−3985.
(30) Ivanova, M. I.; Sievers, S. A.; Sawaya, M. R.; Wall, J. S.; Eisenberg, D. Molecular Basis for Insulin Fibril Assembly. *Proc. Natl. Acad. Sci. U.S.A.* **2009**, *106*, 18990−18995.
(31) Nayak, A.; Sorci, M.; Krueger, S.; Belfort, G. A Universal Pathway for Amyloid Nucleus and Precursor Formation for Insulin. *Proteins* **2009**, *74*, 556−565.
(32) Turnell, W. G.; Finch, J. T. Binding of the Dye Congo Red to the Amyloid Protein Pig Insulin Reveals a Novel Homology Amongst Amyloid-Forming Peptide Sequences. *J. Mol. Biol.* **1992**, *227*, 1205−1223.
(33) Ahmad, A.; Millett, I. S.; Doniach, S.; Uversky, V. N.; Fink, A. L. Partially Folded Intermediates in Insulin Fibrillation. *Biochemistry* **2003**, *42*, 11404−11416.
(34) Ahmad, A.; Uversky, V. N.; Hong, D.; Fink, A. L. Early Events in the Fibrillation of Monomeric Insulin. *J. Biol. Chem.* **2005**, *280*, 42669−42675.
(35) Vestergaard, B.; Groenning, M.; Roessle, M.; Kastrup, J. S.; van de Weert, M.; Flink, J. M.; Frokjaer, S.; Gajhede, M.; Svergun, D. I. A Helical Structural Nucleus Is the Primary Elongating Unit of Insulin Amyloid Fibrils. *PLoS Biol.* **2007**, *5*, 1089−1097.
(36) Podesta, A.; Tiana, G.; Milani, P.; Manno, M. Early Events in Insulin Fibrillization Studied by Time-Lapse Atomic Force Microscopy. *Biophys. J.* **2006**, *90*, 589−597.
(37) Ferrone, F. Analysis of protein aggregation kinetics. *Methods Enzymol.* **1999**, *309*, 256−274.
(38) Dovidchenko, N. V.; Finkelstein, A. V.; Galzitskaya, O. V. How to Determine the Size of Folding Nuclei of Protofibrils from the Concentration Dependence of the Rate and Lag-Time of Aggregation. I. Modeling the Amyloid Protofibril Formation. *J. Phys. Chem. B* **2014**, DOI: 10.1021/jp4083294.
(39) LeVine, H., 3rd. Thioflavine T Interaction with Synthetic Alzheimer's Disease Beta-Amyloid Peptides: Detection of Amyloid Aggregation in Solution. *Protein Sci.* **1993**, *2*, 404−410.
(40) Serpell, L. C.; Fraser, P. E.; Sunde, M. X-Ray Fiber Diffraction of Amyloid Fibrils. *Methods Enzymol.* **1999**, *309*, 526−536.
(41) Khurana, R.; Ionescu-Zanetti, C.; Pope, M.; Li, J.; Nielson, L.; Ramirez-Alvarado, M.; Regan, L.; Fink, A. L.; Carter, S. A. A General Model for Amyloid Fibril Assembly Based on Morphological Studies Using Atomic Force Microscopy. *Biophys. J.* **2003**, *85*, 1135−1144.
(42) Brange, J.; Whittingham, J.; Edwards, D.; You-Shang, Z.; Wollmer, A.; Brandenburg, D.; Dodson, G.; Finch, J. Insulin Structure and Diabetes Treatment. *Curr. Sci.* **1997**, *72*, 470−476.
(43) Glenner, G. G.; Eanes, E. D.; Bladen, H. A.; Linke, R. P.; Termine, J. D. Beta-Pleated Sheet Fibrils. A Comparison of Native Amyloid with Synthetic Protein Fibrils. *J. Histochem. Cytochem.* **1974**, *22*, 1141−1158.
(44) Bouchard, M.; Zurdo, J.; Nettleton, E. J.; Dobson, C. M.; Robinson, C. V. Formation of Insulin Amyloid Fibrils Followed by Ftir Simultaneously with Cd and Electron Microscopy. *Protein Sci.* **2000**, *9*, 1960−1967.
(45) Koltun, W. L.; Waugh, D. F.; Bear, R. S. An X-Ray Diffraction Investigation of Selected Types of Insulin Fibrils. *J. Am. Chem. Soc.* **1954**, *76*, 413−417.
(46) Chiti, F.; Dobson, C. M. Protein Misfolding, Functional Amyloid, and Human Disease. *Annu. Rev. Biochem.* **2006**, *75*, 333−366.
(47) Fodera, V.; Librizzi, F.; Groenning, M.; van de Weert, M.; Leone, M. Secondary Nucleation and Accessible Surface in Insulin Amyloid Fibril Formation. *J. Phys. Chem. B* **2008**, *112*, 3853−3858.
(48) Andersen, C. B.; Yagi, H.; Manno, M.; Martorana, V.; Ban, T.; Christiansen, G.; Otzen, D. E.; Goto, Y.; Rischel, C. Branching in Amyloid Fibril Growth. *Biophys. J.* **2009**, *96*, 1529−1536.
(49) Cohen, S. I.; Linse, S.; Luheshi, L. M.; Hellstrand, E.; White, D. A.; Rajah, L.; Otzen, D. E.; Vendruscolo, M.; Dobson, C. M.; Knowles, T. P. Proliferation of Amyloid-Beta42 Aggregates Occurs through a Secondary Nucleation Mechanism. *Proc. Natl. Acad. Sci. U.S.A.* **2013**, *110*, 9758−9763.
(50) Jeong, J. S.; Ansaloni, A.; Mezzenga, R.; Lashuel, H. A.; Dietler, G. Novel Mechanistic Insight into the Molecular Basis of Amyloid Polymorphism and Secondary Nucleation During Amyloid Formation. *J. Mol. Biol.* **2013**, *425*, 1765−1781.
(51) Hua, Q. X.; Weiss, M. A. Comparative 2d Nmr Studies of Human Insulin and Des-Pentapeptide Insulin: Sequential Resonance Assignment and Implications for Protein Dynamics and Receptor Recognition. *Biochemistry* **1991**, *30*, 5505−5515.
(52) Weiss, M. A.; Nguyen, D. T.; Khait, I.; Inouye, K.; Frank, B. H.; Beckage, M.; O'Shea, E.; Shoelson, S. E.; Karplus, M.; Neuringer, L. J. Two-Dimensional Nmr and Photo-Cidnp Studies of the Insulin Monomer: Assignment of Aromatic Resonances with Application to Protein Folding, Structure, and Dynamics. *Biochemistry* **1989**, *28*, 9855−9873.
(53) Manno, M.; Craparo, E. F.; Podesta, A.; Bulone, D.; Carrotta, R.; Martorana, V.; Tiana, G.; San Biagio, P. L. Kinetics of Different Processes in Human Insulin Amyloid Formation. *J. Mol. Biol.* **2007**, *366*, 258−274.
(54) Nettleton, E. J.; Tito, P.; Sunde, M.; Bouchard, M.; Dobson, C. M.; Robinson, C. V. Characterization of the Oligomeric States of Insulin in Self-Assembly and Amyloid Fibril Formation by Mass Spectrometry. *Biophys. J.* **2000**, *79*, 1053−1065.
(55) Uversky, V. N. Mysterious Oligomerization of the Amyloidogenic Proteins. *FEBS J.* **2010**, *277*, 2940−2953.
(56) Brems, D. N.; Alter, L. A.; Beckage, M. J.; Chance, R. E.; DiMarchi, R. D.; Green, L. K.; Long, H. B.; Pekar, A. H.; Shields, J. E.; Frank, B. H. Altering the Association Properties of Insulin by Amino Acid Replacement. *Protein Eng.* **1992**, *5*, 527−533.